Compact Models Based on Transmission-Line Concept for Integrated Capacitors and Inductors

Kok-Yan Lee, *Member, IEEE*, Saeed Mohammadi, *Senior Member, IEEE*, Pallab K. Bhattacharya, *Fellow, IEEE*, and Linda P. B. Katehi, *Fellow, IEEE*

***Abstract*—This paper presents a compact modeling methodology for inductors and capacitors based on transmission-line theory. Using continued fractions approximation, second- and third-order intrinsic inductor and capacitor models are demonstrated. With the second-order model, one can accurately predict inductor and capacitor behavior up to their first resonance frequencies. With the third-order model, one can match the measured inductor or capacitor response beyond the first resonance frequency. Wideband accurate passive models developed here are essential for transient and harmonic-balance analysis where out-of-band frequencies are important. The model parameters are extracted directly from S-parameter measurement without a need for optimization. Furthermore, the frequency-dependent nonlinear effects of spiral inductors and metal–insulator–metal capacitors are expressed based on simple models without resorting to frequency-dependent parameters.**

***Index Terms*—Equivalent-circuit model, integrated passives, lumped elements, metal–insulator–metal (MIM) capacitors, quality factor, self-resonance, spiral inductors.**

I. Introduction

INTEGRATED metal–insulator–metal (MIM) capacitors and spiral inductors are important components of RF circuits. While MIM capacitors present parasitic effects at high frequencies, integrated inductors suffer from a poor quality factor Q and low self-resonance frequency $f_{\rm sr}$. Efforts to improve Q and $f_{\rm sr}$ of integrated inductors are widely reported in the literature [1]–[8]. For accurate time-domain analysis, as well as nonlinear harmonic-balance analysis, it is necessary to analyze and model both inductors and capacitors up to very high frequencies and sometimes beyond their respective self-resonance frequencies.

Inductor analysis and design have been described by experimental means [9], electromagnetic (EM) simulations [10], or approximating formulas [11]–[14]. Most of these approximations are based on a comprehensive collection of formulas by Grover [15] or the algorithm for computing inductance of planar rectangular spirals by Greenhouse [16].

In addition to design equations, it is also important to develop inductor models verified against measured results to construct design libraries in computer-aided design (CAD) simulation environments. The most common inductor model is the standard π-model with frequency-independent lumped elements [14], [17]. While this model is useful over a limited frequency range, it does not properly model the distributed effects, proximity effects, or the higher order loss effects such as the conductor skin effect, current crowding, capacitive coupling, and eddy current. A conventional π-model has been extended with frequency-dependent lumped elements [2], [14], [18], [19]. The resulting models do a better job of describing the higher order frequency effects, but cannot be easily implemented in time-domain simulators. There are also alternative models that try to address the high-frequency effects [9], [14], [20], [21]. These models are not widely utilized in CAD simulators.

Most capacitor models use standard series circuit. More complicated models including distributed and π-models for capacitors have also been proposed [2], [22]–[27].

This paper presents a new comprehensive modeling methodology for integrated inductors and capacitors based on a transmission-line concept [28]. The third-order and higher order inductor and capacitor models developed here provide an accurate response beyond the first self-resonance frequency without the need for complicated optimization-based extraction. The models are very simple, flexible, and consist entirely of ideal frequency-independent lumped elements suitable for time-domain transient analysis (SPICE) or harmonic-balance nonlinear simulation. Model parameters are extracted from S-parameter data in an unambiguous manner without the need for optimization. This allows the designer to have an insight into the limitation and design parameters of integrated passive elements.

Model development for both integrated inductors and capacitors is described in Section II, while parameter-extraction techniques are discussed in Section III. Section IV provides discussions and concluding remarks.

II. Model Development

To develop an accurate model, it is necessary to extract the extrinsic shunt pad/parasitic capacitances of either an inductor or capacitor using a standard π-model. Although only inductor modeling is shown, the capacitor model can be easily found by substituting $Y_{\rm ind}$ with $Y_{\rm cap}$ (or $Z_{\rm ind}$ with $Z_{\rm cap}$). First, two-port measured S-parameter data are transformed to an $ABCD$ matrix. The relation between the $ABCD$ matrix and components of the π-model is given by

$$ABCD_{\rm full} = \begin{bmatrix} 1+\dfrac{Y_{\rm ext2}}{Y_{\rm ind}} & \dfrac{1}{Y_{\rm ind}} \\ Y_{\rm ext1}+Y_{\rm ext2}+\dfrac{Y_{\rm ext1}Y_{\rm ext2}}{Y_{\rm ind}} & 1+\dfrac{Y_{\rm ext1}}{Y_{\rm ind}} \end{bmatrix} \quad (1)$$

Manuscript received February 17, 2006; revised July 19, 2006.

K.-Y. Lee and P. K. Bhattacharya are with the Department of Electrical Engineering and Computer Science, The University of Michigan at Ann Arbor, Ann Arbor, MI 48109 USA (e-mail: kokyan@ieee.org; pkb@eecs.umich.edu).

S. Mohammadi is with the School of Electrical and Computer Engineering, Purdue University, West Lafayette, IN 47907-2035 USA (e-mail: saeedm@purdue.edu).

L. P. B. Katehi is with the Office of the Provost, University of Illinois at Urbana-Champaign, Urbana, IL 61820 USA (e-mail: katehi@uiuc.edu).

Digital Object Identifier 10.1109/TMTT.2006.886157

where Y_{ext1} and Y_{ext2} are the shunt extrinsic admittance at ports 1 and 2, respectively, and $Z_{\text{ind}} = 1/Y_{\text{ind}}$ is the impedance of the intrinsic inductor and $Y_{\text{cap}} = 1/Z_{\text{cap}}$ is the admittance of the intrinsic capacitor to be modeled. Using (1), one can unambiguously extract extrinsic admittances of the passive device. It also allows us to work on the intrinsic inductor (or capacitor) model through the B-parameter of the $ABCD_{\text{full}}$ matrix using the following equations:

$$Z_{\text{ind}} = B_{\text{full}} \quad Y_{\text{ext1}} = \frac{D_{\text{full}} - 1}{B_{\text{full}}} \quad Y_{\text{ext2}} = \frac{A_{\text{full}} - 1}{B_{\text{full}}}. \quad (2)$$

Next, the intrinsic inductor found from (2) is modeled as an ideal short-circuit transmission line. For capacitors, an ideal open-circuit transmission line is used. The short- or open-circuit transmission-line equations are then approximated using the first-, second-, or third-order continued fractions approximation of $\tanh(\gamma l)$ and translated into traditional equivalent circuits to obtain the first-, second-, or third-order intrinsic inductor and capacitor models. The model could easily be extended further to a fourth order, if necessary, to model the passive device beyond the second resonance.

The input impedance Z_{in} of a transmission line can be described by

$$Z_{\text{in}} = \frac{Z_L + Z_0 \tanh(\gamma l)}{Z_0 + Z_L \tanh(\gamma l)} Z_0 \quad (3)$$

where l is the length of the transmission line (actual value is not needed), Z_L is the load impedance, and Z_0 and γ are the characteristic impedance and complex propagation constant of the transmission line, respectively. Substituting $Z_L = 0$ for an ideal short-circuit termination for inductors or $Z_L = \infty$ for an ideal open-circuit termination for capacitors results in

$$Z_{\text{ind}} = Z_0 \tanh(\gamma l) \quad Y_{\text{cap}} = Y_0 \tanh(\gamma l). \quad (4)$$

Expansion of $\tanh(\gamma l)$ using the continued fractions approximation given by [29]

$$\tanh(\gamma l) = \cfrac{(\gamma l)}{1 + \cfrac{(\gamma l)^2}{3 + \cfrac{(\gamma l)^2}{5 + \cdots}}} \quad (5)$$

where

$$\gamma = \sqrt{(R + j\omega L)(G + j\omega C)} \quad Z_0 = \sqrt{\frac{(R + j\omega L)}{(G + j\omega C)}} \quad (6)$$

allows for very simple translation into an equivalent-circuit model. In the above equation, C is the shunt capacitance per unit length in farads per meter, L is the series inductance per unit length in henrys per meter, R is the series resistance per unit length in ohms per meter, G is the shunt conductance per unit length in siemens per meter, and l is the length of the transmission line.

By substituting (5) and (6) in (4), we are able to obtain the first-, second-, and third-order approximation of the intrinsic inductor impedance Z_{ind} (capacitance admittance Y_{cap}). The first-order approximation of the inductor impedance Z_{ind} results in a simple series *RL* network. First-order approximation of the capacitor admittance Y_{cap} results in a shunt *RC* network.

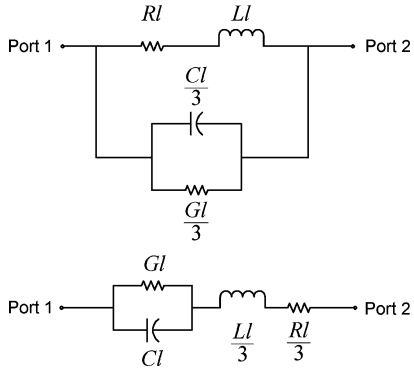

Fig. 1. Second-order transmission-line circuit models of: (*top*) inductor and (*bottom*) capacitor.

The second-order approximations of the inductor admittance Y_{ind} and capacitor impedance Z_{cap} are

$$Y_{\text{ind}} = \frac{1}{Rl + j\omega Ll} + \frac{Gl + j\omega Cl}{3} \quad (7)$$

$$Z_{\text{cap}} = \frac{1}{Gl + j\omega Cl} + \frac{Rl + j\omega Ll}{3}. \quad (8)$$

where the equivalent-circuit models are shown in Fig. 1.

The third-order approximation of the inductor input impedance Z_{ind} is

$$Z_{\text{ind}} = \frac{1}{Y_1 + Y_2}$$

where

$$Y_1 = \frac{1}{Rl + j\omega Ll}$$
$$Y_2 = \frac{1}{Z_3 + Z_4}$$
$$Z_3 = \frac{3}{(Gl + j\omega Cl)}$$
$$Z_4 = \frac{1}{5}(Rl + j\omega Ll). \quad (9)$$

The third-order approximation of the capacitor input impedance Z_{cap} is

$$Z_{\text{cap}} = Z_1 + Z_2$$

where

$$Y_1 = Gl + j\omega Cl$$
$$Y_2 = Y_3 + Y_4$$
$$Z_3 = \frac{1}{3}(Rl + j\omega Ll)$$
$$Y_4 = \frac{1}{5}(Gl + j\omega Cl). \quad (10)$$

The equivalent-circuit models of inductors and capacitors using the third-order approximation are shown in Fig. 2.

III. Parameter Extraction

Using a standard microfabrication process on high-resistivity Si, we fabricated three different inductors (1.5, 3.5, and 4.5

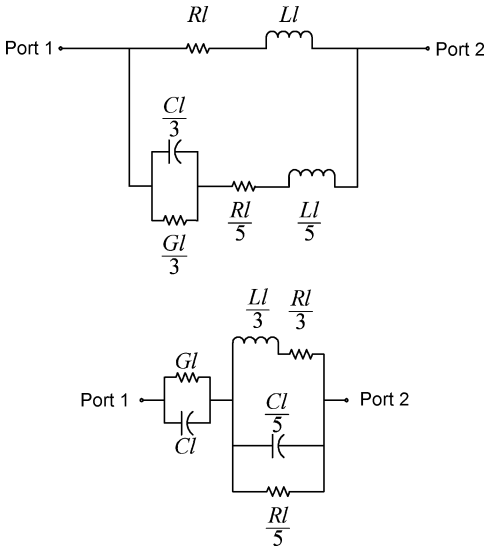

Fig. 2. Third-order transmission-line circuit models of: (*top*) inductor and (*bottom*) capacitor.

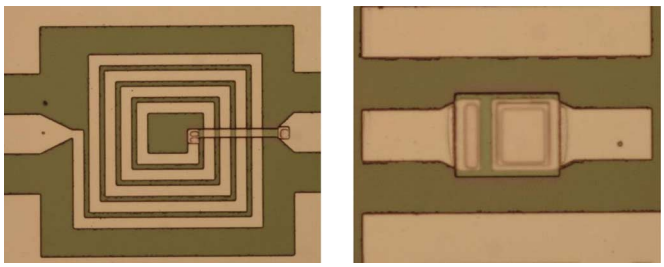

Fig. 3. Photomicrograph of fabricated 4.5-turn spiral inductor (*left*) and 6000-μm^2 MIM capacitor (*right*). (Color version available online at http://ieee-explore.ieee.org.)

turns) and three different capacitors (with areas of 1000, 3000, and 6000 μm^2). A two-metal process with vias through silicon dioxide was used to fabricate inductors and capacitors. A 1-μm lower metal layer (Ti/Au) was used as an underpass for the inductors and lower metal plate for the capacitors. A 2-μm top metal layer (Ti/Au) was used for spiral winding, as well as the capacitor top metal plate. The thickness of SiO_2 separating the two inductor metal layers was 7500 Å, while the SiO_2 dielectric thickness was 2500 Å for the capacitors. Fig. 3 shows fabricated inductors and capacitors in this technology.

On-wafer two-port S-parameter measurement was used to characterize the inductors and capacitors up to 26 GHz. The S-parameter data was converted to an $ABCD$ matrix and intrinsic and extrinsic admittances $Y_{\rm cap}$, $Y_{\rm ind}$, $Y_{\rm ext1}$, and $Y_{\rm ext2}$ as a function of frequency were extracted using (2).

A. Second-Order Intrinsic Inductor and Capacitor Models

Here, we will describe the procedure to obtain all the model parameters for the second-order intrinsic inductor and capacitor models. Note that no optimization is used to achieve these results. The procedure relies on linearizing both the real and imaginary part of the admittance (impedance) of the second-order intrinsic inductor (capacitor) model. The linearization approximation becomes more accurate as the frequency increases. For the second-order inductor model shown in Fig. 1 and described by (7), one finds that

$$\mathrm{Re}(Y_{\rm ind}) = G_d + \frac{1/R_c}{1+(\omega L_{\rm ind}/R_c)^2} \tag{11a}$$

$$\mathrm{Im}(Y_{\rm ind}) = -\omega\left[\frac{L_{\rm ind}/R_c^2}{1+(\omega L_{\rm ind}/R_c)^2} - C_{\rm ind}\right] \tag{11b}$$

where $L_{\rm ind} = Ll$, $C_{\rm ind} = Cl/3$, $R_d = 1/G_d = 3/(Gl)$, and $R_c = Rl$. By assuming that $(\omega L_{\rm ind}/R_c)^2 \gg 1$, we can linearize (11) as

$$\mathrm{Re}(Y_{\rm ind}) \approx \frac{R_c}{L_{\rm ind}^2}\frac{1}{\omega^2} + \frac{1}{R_d} \tag{12a}$$

$$\frac{\mathrm{Im}(Y_{\rm ind})}{\omega} \approx -\frac{1}{L_{\rm ind}}\frac{1}{\omega^2} + C_{\rm ind}. \tag{12b}$$

Note that accurate model parameters can be extracted from the frequencies that meet the criteria of $(\omega L_{\rm ind}/R_c)^2 \gg 1$ and is below the first resonance frequency. Similarly, Fig. 1 and (8) can be used to find the second-order parameter models of a capacitor. The assumption of $(\omega R_d C_{\rm cap})^2 \gg 1$, which is more accurate at higher frequencies, results in unambiguous extraction of the capacitor model parameters as

$$\mathrm{Re}(Z_{\rm cap}) \approx \frac{1}{R_d C_{\rm cap}^2}\frac{1}{\omega^2} + R_c \tag{13a}$$

$$\frac{\mathrm{Im}(Z_{\rm cap})}{\omega} \approx -\frac{1}{C_{\rm cap}}\frac{1}{\omega^2} + L_{\rm cap}. \tag{13b}$$

Equations (12) and (13) can be plotted as functions of angular frequency ω to determine second-order model parameters of measured inductors and capacitors. Fig. 4 shows the extraction technique for three different inductors, while Fig. 5 depicts the extraction of the second-order model parameters of three different capacitors. Note that the fitting of these parameters is done at relatively high frequencies, but still below the first self-resonance frequency of the device. A simple two-point linear approximation or a least squares linear approximation could be used to approximate the straight line and extract the model parameters.

The imaginary parts of the admittances of the inductors (impedances of the capacitors) shown in Fig. 4 (Fig. 5) depict very linear characteristics, which result in accurate extraction of $L_{\rm ind}$ and $C_{\rm ind}$ ($L_{\rm cap}$ and $C_{\rm cap}$), but the real part of the inductor admittances (capacitor impedances) are not linear at higher frequencies (low $1/\omega^2$). Therefore, the second-order model does not accurately predict losses (R_d, R_c, and, therefore, Q) of inductors and capacitors at very high frequencies and beyond the first resonance frequency.

B. Third-Order Intrinsic Inductor and Capacitor Models

Here, we will describe the extraction of the third-order inductor and capacitor models without optimization. The procedure is an extension to the second-order model parameter extraction described above and requires parameter values extracted from the second-order models that are used in the third-order model equations.

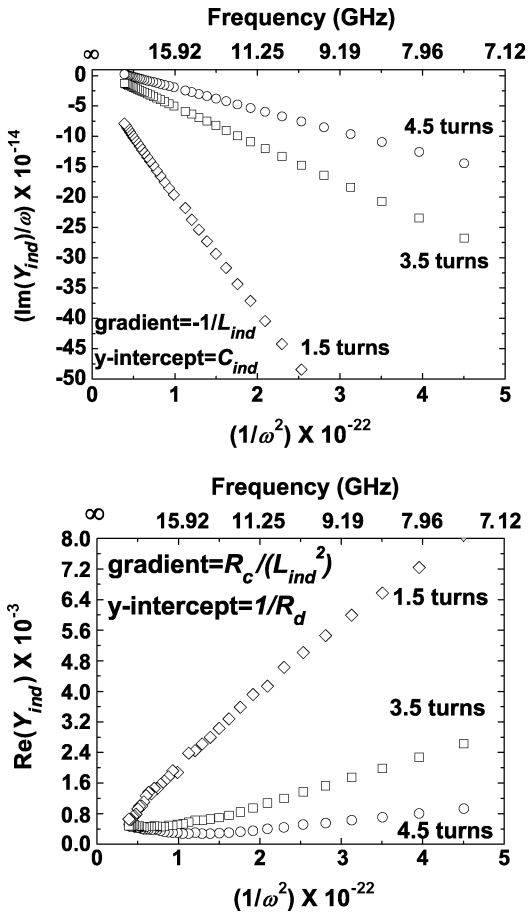

Fig. 4. Graphical method to extract: (*top*) $L_{\rm ind}$ and $C_{\rm ind}$ and (*bottom*) R_d and R_c of three different inductors from $Y_{\rm ind}$. $Y_{\rm ind}$ is extracted from S-parameter measurements according to (2).

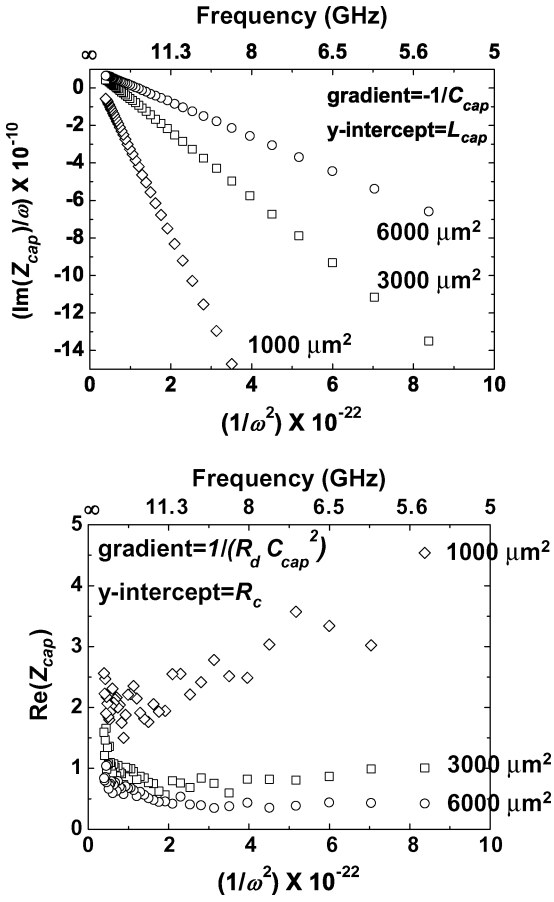

Fig. 5. Graphical method to extract: (*top*) $L_{\rm cap}$ and $C_{\rm cap}$ and (*bottom*) R_d and R_c of three different capacitors from $Z_{\rm cap}$. $Z_{\rm cap}$ is extracted from S-parameter measurements according to (2) by substituting $Y_{\rm ind}$ with $Z_{\rm cap}$.

Starting from the standard third-order inductor model, as shown in Fig. 2 and (9), we can obtain Y_2 as

$$Y_2 = Y_{\rm ind} - \frac{1}{R_c + j\omega L_{\rm ind}}. \tag{14}$$

This equation can be rewritten as

$$\mathrm{Re}(Z_2) = R_{\rm 3rd\_order} + \frac{R_d}{1+(\omega R_d C_{\rm ind})^2} \tag{15a}$$

$$\frac{\mathrm{Im}(Z_2)}{\omega} = L_{\rm 3rd\_order} - \frac{R_d^2 C_{\rm ind}}{1+(\omega R_d C_{\rm ind})^2}. \tag{15b}$$

Again, by assuming that $(\omega R_d C_{\rm ind})^2 \gg 1$, we can approximate (15) with the following:

$$\mathrm{Re}(Z_2) \approx R_{\rm 3rd\_order} + \frac{1}{R_d C_{\rm ind}^2}\frac{1}{\omega^2} \tag{16a}$$

$$\frac{\mathrm{Im}(Z_2)}{\omega} \approx L_{\rm 3rd\_order} - \frac{1}{C_{\rm ind}}\frac{1}{\omega^2}. \tag{16b}$$

The model parameters are extracted from the frequencies where the assumption of $(\omega R_d C_{\rm ind})^2 \gg 1$ is valid. Using (16) and plotting, one can extract the third-order parameters as shown in Fig. 6.

Similarly, Fig. 2 and (10) can be used to find the third-order parameter models of a capacitor. The assumption of $(\omega L_{\rm cap}/R_c)^2 \gg 1$ results in an unambiguous extraction of the third-order capacitor model parameters as

$$\mathrm{Re}(Y_2) \approx \frac{1}{R_{3rd}} + \frac{R_c}{L_{\rm cap}^2}\frac{1}{\omega^2} \tag{17a}$$

$$\frac{\mathrm{Im}(Y_2)}{\omega} \approx C_{3rd} - \frac{1}{L_{\rm cap}}\frac{1}{\omega^2}. \tag{17b}$$

The model parameters are extracted from the frequencies where the assumption of $(\omega L_{\rm cap}/R_c)^2 \gg 1$ is valid.

In fact, the third-order parameters should be extracted from frequencies above the first resonance frequency and below the second resonance frequency.

The extrinsic admittances $Y_{\rm ext1}$ and $Y_{\rm ext2}$ can be accurately modeled using second-order capacitance models, as described in Section III-A.

Table I lists the final parameter values of the inductor models studied here. The 4.5-turn inductor and the 3.5-turn inductor uses the third-order intrinsic inductor model and the second-order extrinsic capacitance model. The 1.5-turn inductor is accurately modeled by the first-order intrinsic inductor model and second-order extrinsic capacitance model. This is due to the fact that the self-resonance frequency of the 1.5-turn

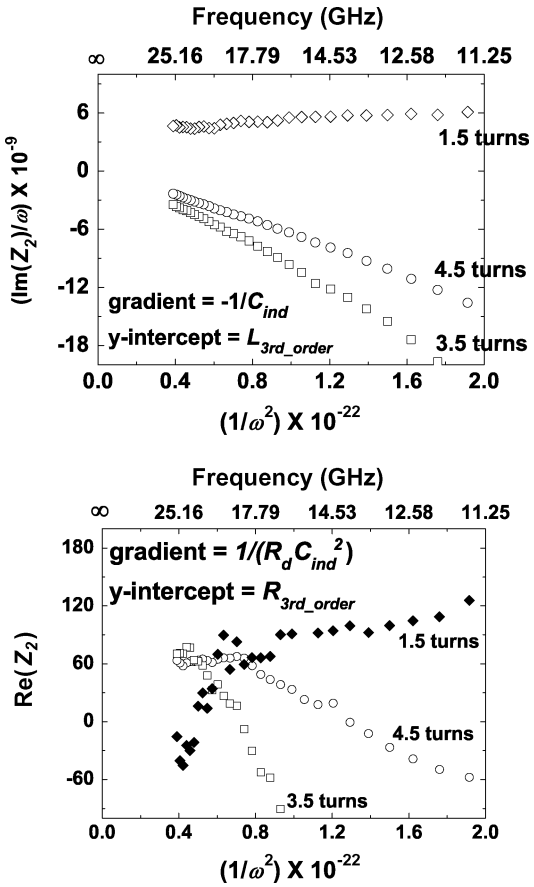

Fig. 6. Graphical method to extract: (*top*) $L_{3\text{rd\_order}}$ and C_{ind} and (*bottom*) $R_{3\text{rd\_order}}$ and R_d by fitting the intermediate data to straight line equations.

TABLE I
COMPLETE MODEL PARAMETERS FOR SPIRAL INDUCTORS FABRICATED AND CHARACTERIZED IN THIS STUDY

Model parameters	4.5 turns	3.5 turns	1.5 turns
2nd order C_{ind} fF	14.35	12.51	-3.71
3rd order C_{ind} fF	14.58	12.58	-
L_{ind} nH	2.83	1.59	0.51
2nd order R_d kΩ	-18.42	-48.74	-7.26
3rd order R_d kΩ	-5.19	-3.55	-
R_c Ω	17.52	13.93	5.38
R_{3rd_order} Ω	113.58	160.99	-
L_{3rd_order} nH	0.29	-0.12	-
Input C_{ext} fF	40.32	29.61	15.63
Input L_{ext} nH	0.27	0.19	-0.05
Input R_{d_ext} kΩ	5.94	5.74	893.72
Input R_{c_ext} Ω	3.19	2.38	19.16
Output C_{ext} fF	30.34	24.31	16.36
Output L_{ext} nH	0.035	0.10	-0.06
Output R_{d_ext} kΩ	-9.75	-3.94	15.14
Output R_{c_ext} Ω	3.75	11.31	17.07

inductor studied here is above 26 GHz, which was the maximum measured frequency. The complete third-order inductor model with second-order extrinsic admittance models is shown in Fig. 7.

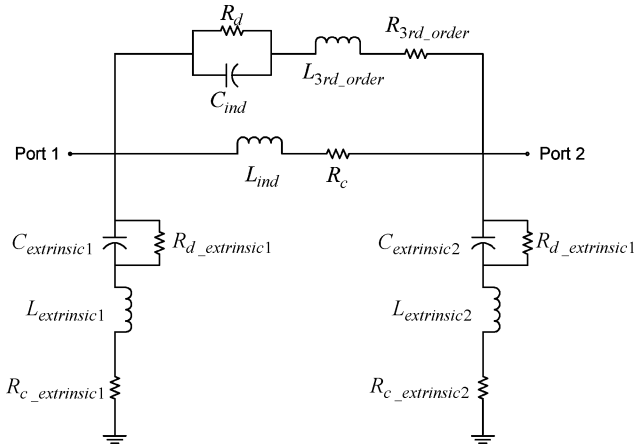

Fig. 7. Complete third-order inductor model with second-order model for extrinsic admittances.

TABLE II
COMPLETE MODEL PARAMETERS FOR MIM CAPACITORS FABRICATED AND CHARACTERIZED IN THIS STUDY

Model parameters	6000 μm^2	3000 μm^2	1000 μm^2
2nd order L_{cap} nH	0.105	0.118	0.119
2nd order C_{cap} pF	1.099	0.571	0.222
C_{3rd_order} fF	4.946	7.746	0.244
2nd order R_c Ω	0.265	0.618	1.503
2nd order R_d kΩ	4.395	8.247	9.021
R_{3rd_order} kΩ	0.562	0.397	24.9
Input C_{ext} fF	37.89	25.5	18.6
Input R_{ext} Ω	50	50	0
Output C_{ext} fF	5.367	4.5	4.3
Output R_{ext} Ω	0	25	0

The negative R_d resistance is shown for completeness. They are the result of inaccurate calibration/deembedding, measurement, and extraction. These resistors should be left as ∞ since they are in shunt with femtofarad capacitances. This means that only at much higher frequency than what was measured will the impedance of the R_d resistor be significant enough to measure accurately.

The third-order intrinsic capacitance model can be found using a similar approach taken for inductors, as described above. The model parameters extracted from S-parameters are shown in Table II. For these capacitors, it was sufficient to use a third-order intrinsic capacitor model combined with first-order extrinsic admittance models, as shown in Fig. 8.

IV. DISCUSSION AND CONCLUSION

Fig. 9 compares the measured S-parameters of a representative capacitor and inductor with their models, while Fig. 10 compares the measured input impedances of the inductors with their complete equivalent-circuit models. Fig. 11 compares the measured input admittances of the capacitors with their complete equivalent-circuit models. It is also interesting to study the quality factor Q of these devices specially the inductors. The quality factor of an inductor is defined as the ratio of the magnetic energy stored in the inductor to the energy dissipated. It

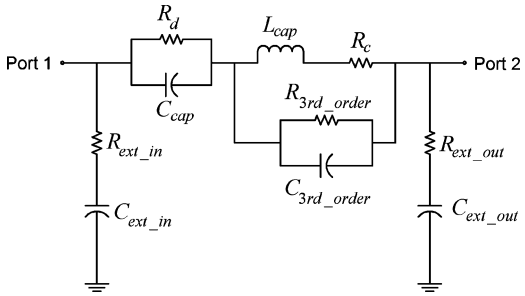

Fig. 8. Complete third-order capacitor model with first-order model for extrinsic admittances.

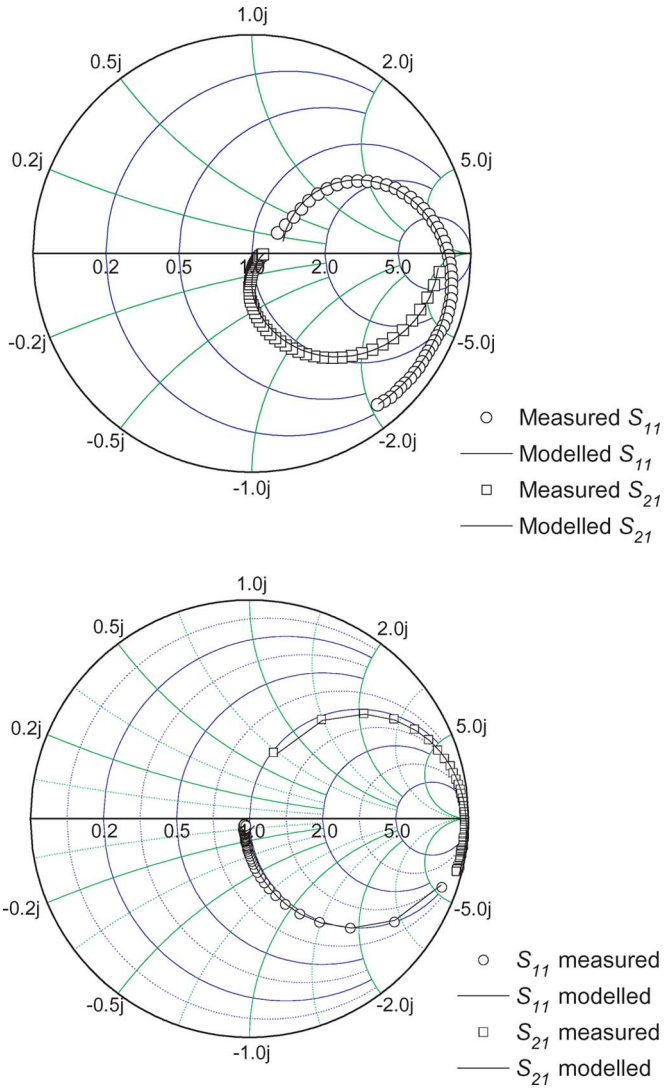

Fig. 9. Comparison of the measured and modeled S-parameters across 0.05–26 GHz for a 4.5-turn inductor (*top*) and a 6000-μm^2 capacitor (*bottom*). (Color version available online at http://ieeexplore.ieee.org.)

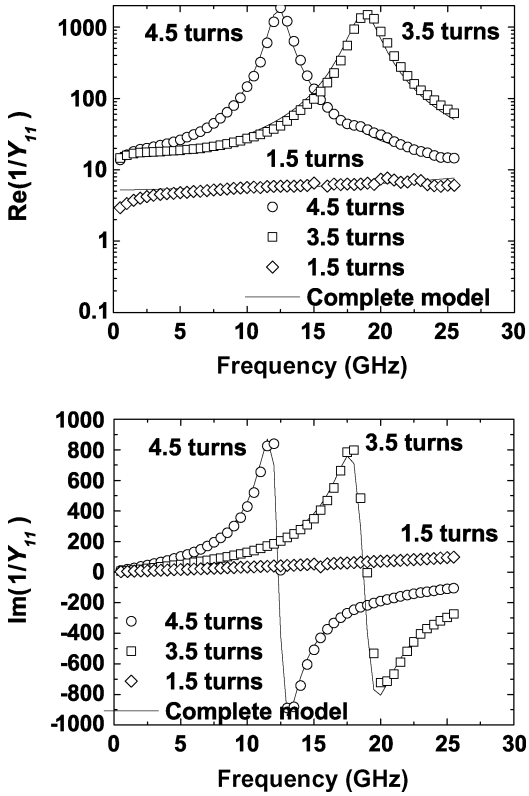

Fig. 10. Measured and modeled input impedance of inductors studied here.

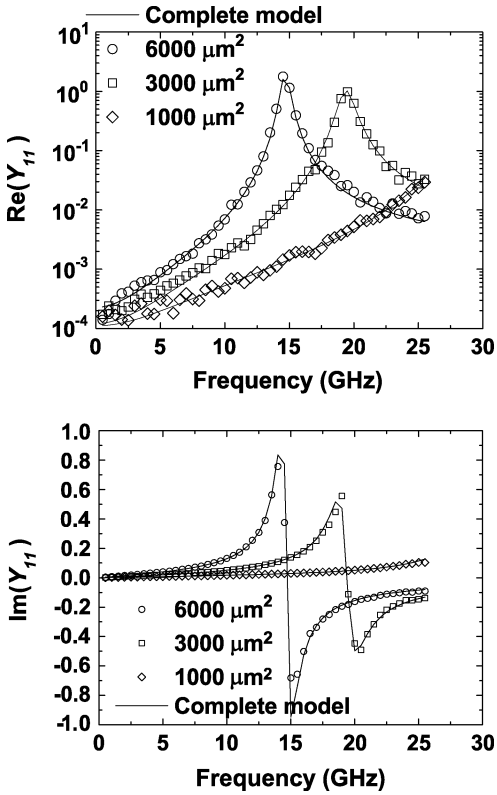

Fig. 11. Measured and modeled input admittance of capacitors studied here.

is often hard to model Q of the inductor as the energy dissipation term is frequency dependent due to multiple loss effects (eddy current, skin effect, and current crowding). Additionally, for high-Q inductors, the dissipated energy is very small and, thus, errors in the measurement can result in inaccurate models. Fig. 12 depicts the modeled and measured quality factor of the 4.5-turn inductor studied here using both second- and third-order models. Notice that with the third-order model, we are able to match the factor beyond the first resonance frequency

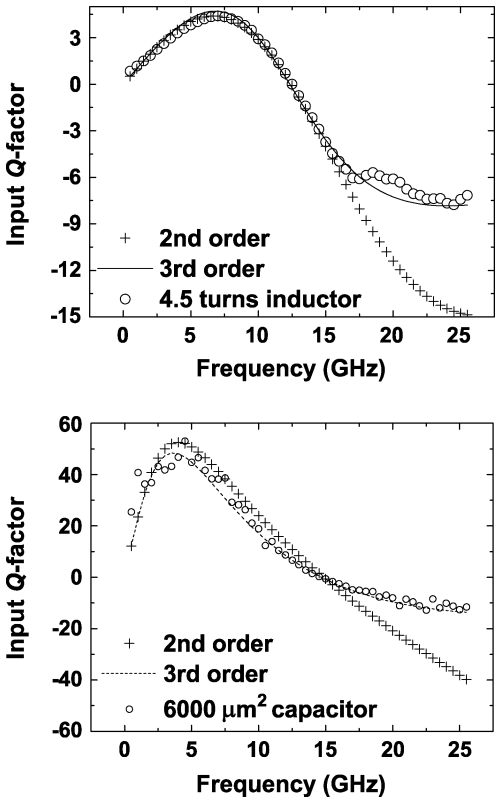

Fig. 12. Measured and modeled input quality factor of 4.5-turn inductor (*top*) and a 6000-μm^2 capacitor (*bottom*).

where the inductor behaves like a capacitor. The second-order model matches the measured inductors up to the first self-resonance frequency where distributed frequency-dependent loss effects can still be ignored. Similar conclusions could be made with the 6000-μm^2 capacitor.

In conclusion, we have demonstrated a new modeling methodology for integrated spiral inductors and MIM capacitors based on fundamental transmission-line theory and continued fractions approximation. The model can be expressed either based on a second- or third-order approximation of shorted (or open-circuited) transmission-line impedance (admittance), which is a hyperbolic tangent function. As the model originates from a lossy transmission-line equation and is approximated using continued fraction approximation of a tanh equation, it can be very accurate and wideband. The second-order model can be extracted easily and is valid up to the self-resonance frequency of the passive component. The third-order model is able to accurately predicts the measured results of passive components beyond their first resonance frequency without any need for optimization. The wideband accuracy provided by our approach is shown in modeling the quality factor of inductors. The accurate wideband model for passive components is instrumental in transient response simulation and also in cases where the harmonic frequency response is important. This modeling methodology can very easily be extended to fourth or higher orders if necessary. The parameter-extraction technique discussed here for both second- and third-order models does not require any optimization and could be implemented using least squares linear approximation resulting in an unambiguous model construction.

REFERENCES

[1] R. A. Johnson, C. E. Chang, P. M. Asbeck, M. E. Wood, G. A. Garcia, and I. Lagnado, "Comparison of microwave inductors fabricated on silicon-on-sapphire and bulk silicon," *IEEE Microw. Guided Wave Lett.*, vol. 6, no. 9, pp. 323–325, Sep. 1996.

[2] J. N. Burghartz, M. Soyuer, and K. A. Jenkins, "Microwave inductors and capacitors in standard multilevel interconnect silicon technology," *IEEE Trans. Microw. Theory Tech.*, vol. 44, no. 1, pp. 100–104, Jan. 1996.

[3] W. B. Kuhn, X. He, and M. Mojarradi, "Modeling spiral inductors in SOS processes," *IEEE Trans. Electron Devices*, vol. 51, no. 5, pp. 677–683, May 2004.

[4] R. Ramachandran, D. Newlin, and A. Pham, "Development of RF/microwave on-chip inductors using an organic micromachining process," in *IEEE 10th Elect. Performance Electron. Packag. Top. Meeting Dig.*, 2001, pp. 97–100.

[5] L. H. Lu, G. E. Ponchak, P. Bhattacharya, and L. P. B. Katehi, "High-Q X-band and K-band micromachined spiral inductors for use in Si-based integrated circuits," in *IEEE MTT-S Int. Microw. Symp. Dig.*, 2000, pp. 108–112.

[6] M. C. Hsieh, Y. K. Fang, C. H. Chen, S. M. Chen, and W. K. Yeh, "Design and fabrication of deep submicron CMOS technology compatible suspended high-Q spiral inductors," *IEEE Trans. Electron Devices*, vol. 51, no. 3, pp. 324–331, Mar. 2004.

[7] D. H. Weon, J. H. Jeon, J. I. Kim, S. Mohammadi, and L. P. B. Katehi, "High-Q integrated 3-D inductors and transformers for high frequency applications," in *IEEE MTT-S Int. Microw. Symp. Dig.*, Jun. 2004, pp. 877–880.

[8] C. P. Yue and S. S. Wong, "On-chip spiral inductors with patterned ground shields for Si-based RF IC's," *IEEE J. Solid-State Circuits*, vol. 33, no. 5, pp. 743–752, May 1998.

[9] I. J. Bahl, "High-performance inductors," *IEEE Trans. Microw. Theory Tech.*, vol. 49, no. 4, pp. 654–664, Apr. 2001.

[10] F. Ling, J. Song, T. Kamgaing, Y. Yang, W. Blood, M. Petras, and T. Myers, "Systematic analysis of inductors on silicon using EM simulations," in *Electron. Compon. Technol. Conf.*, 2002, pp. 484–489.

[11] H. A. Wheeler, "Simple inductance formulas for radio coils," *Inst. Radio Eng.*, vol. 16, no. 10, pp. 1398–1400, Oct. 1928.

[12] C. P. Yue, C. Ryu, J. Lau, T. H. Lee, and S. S. Wong, "A physical model for planar spiral inductors on silicon," in *IEEE Int. Electron. Device Meeting Tech. Dig.*, 1996, pp. 155–158.

[13] C. P. Yue and S. S. Wong, "Physical modeling of spiral inductors on silicon," *IEEE Trans. Electron Devices*, vol. 47, no. 3, pp. 560–568, Mar. 2000.

[14] J. R. Long and M. A. Copeland, "The modeling, characterization, and design of monolithic inductors for silicon RF IC's," *IEEE J. Solid-State Circuits*, vol. 32, no. 3, pp. 357–369, Mar. 1997.

[15] F. W. Grover, *Inductance Calculations*. New York: Van Nostrand, 1946.

[16] H. M. Greenhouse, "Design of planar rectangular microelectronic inductors," *IEEE Trans. Parts, Hybrids, Packag.*, vol. PHP-10, no. 2, pp. 101–109, Jun. 1974.

[17] N. M. Nguyen and R. G. Meyer, "Si IC-compatible inductors and *LC* passive filters," *IEEE J. Solid-State Circuits*, vol. 25, no. 4, pp. 1028–1031, Aug. 1990.

[18] E. Pettenpaul, H. Kapusta, A. Weisgerber, H. Mampe, J. Luginsland, and I. Wolff, "CAD models of lumped elements on GaAs up to 18 GHz," *IEEE Trans. Microw. Theory Tech.*, vol. 36, no. 2, pp. 294–304, Feb. 1988.

[19] J. R. Long and M. A. Copeland, "Modeling of monolithic inductors and transformers for silicon RFIC design," in *IEEE MTT-S Int. Microw. Symp. Dig.*, 1995, pp. 129–134.

[20] L. Heinemann, R. Schulze, P. Wallmeier, and H. Grotstollen, "Modeling of high frequency inductors," in *IEEE Power Electron. Specialists Conf.*, 1994, vol. 2, pp. 876–883.

[21] T. Kamgaing, T. Myers, M. Petras, and M. Miller, "Modeling of frequency dependent losses in two-port and three-port inductors on silicon," in *IEEE Radio Freq. Integr. Circuits Symp.*, 2002, pp. 307–310.

[22] C. C. Kuo, M. Y. Kuo, and M. S. Kuo, "Modeling of capacitors and nonlinear inductors using piecewise curve fitting technique," in *IEEE 4th Comput. in Power Electron. Workshop*, 1994, pp. 133–138.

[23] S. Saimi, C. Joubert, and C. Glaize, "High frequency model for power electronics capacitors," *IEEE Trans. Power Electron.*, vol. 16, no. 2, pp. 157–166, Mar. 2001.

[24] B. Lakshminarayanan, H. C. Gordon, and T. M. Weller, "A substrate-dependent CAD model for ceramic multilayer capacitors," *IEEE Trans. Microw. Theory Tech.*, vol. 48, no. 10, pp. 1687–1693, Oct. 2000.
[25] R. A. Pucel, "Design considerations for monolithic microwave circuits," *IEEE Trans. Microw. Theory Tech.*, vol. MTT-29, no. 6, pp. 513–534, Jun. 1981.
[26] W. Z. Cai, S. C. Shastri, M. Azam, C. Hoggatt, G. H. Loechelt, G. M. Grivna, Y. Wen, and S. Dow, "Development and extraction of high-frequency spice models for metal-insulator-metal capacitors," in *Proc. IEEE Int. Microelectron. Test Structures Conf.*, Mar. 2004, vol. 17, pp. 231–234.
[27] S. S. Song, S. W. Lee, J. Gil, and H. Shin, "Simple wideband metal–insulator–metal (MIM) capacitor model for RF applications and effect of substrate grounded shields," *Japn. J. Appl. Phys.*, vol. 43, no. 4B, pp. 1746–1751, 2004.
[28] K. Lee, S. Mohammadi, P. K. Bhattacharya, and L. P. B. Katehi, "Scalable compact models for embedded passives," presented at the Eur. Microw. Conf., Oct. 4–6, 2005.
[29] M. Abramowitz and I. A. Stegun, *Handbook of Mathematical Functions With Formulas, Graphs, and Mathematical Tables*. Washington, DC: U.S. Dept. Commerce, 1972.

Kok-Yan Lee (S'99–M'05) received the B.Eng. degree (Hons.) from Nanyang Technological University, Nanyang, China, in 1995, and the M.Eng. and Ph.D. degrees in electrical engineering from The University of Michigan at Ann Arbor, in 2001 and 2005, respectively.

Since 1991, he has been with DSO National Laboratories, Singapore, initially as a Technical Officer and currently as a Senior Member of Technical Staff. His research interests include microelectromechanical systems (MEMS) process and circuit applications, SiGe-based monolithic-microwave integrated-circuit (MMIC) process, device modeling, and circuit design.

Dr. Lee was the recipient of the 1986 National Youth Service Award in Science and Technology (Group Award).

Saeed Mohammadi (S'89–M'92–SM'02) received the Ph.D. degree in electrical engineering from The University of Michigan at Ann Arbor, in 2000.

He is currently an Assistant Professor of electrical and computer engineering with Purdue University, West Lafayette, IN, where his group is currently involved in research on RF devices and circuits, RF packaging, and nanoelectronic technology. He has authored or coauthored over 60 journal and refereed conference papers in these areas.

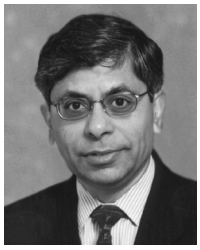

Pallab K. Bhattacharya (M'78–SM'83–F'89) received the Ph.D. degree from the University of Sheffield, Sheffield, U.K., in 1978.

He is the Charles M. Vest Distinguished University Professor of Electrical Engineering and Computer Science and the James R. Mellor Professor of Engineering with the Department of Electrical Engineering and Computer Science, The University of Michigan at Ann Arbor. He is Editor-in-Chief of the *Journal of Physics D*. He edited *Properties of Lattice-Matched and Strained InGaAs* (INSPEC, 1993) and *Properties of III-V Quantum Wells and Superlattices* (INSPEC, 1996). He also authored the textbook *Semiconductor Optoelectronic Devices* (Prentice-Hall, 1996, 2nd ed.). His teaching and research interests are compound semiconductors, low-dimensional quantum confined systems, nanophotonics, and opto-electronic integrated circuits.

Prof. Bhattacharya is a Fellow of the American Physical Society, the Institute of Physics (UK), and the Optical Society of America (OSA). He was an editor for the IEEE TRANSACTIONS ON ELECTRON DEVICES. He was the recipient of the John Simon Guggenheim Fellowship, the IEEE Electron Device Society Paul Rappaport Award, the IEEE Lasers and Electro-Optics Society Engineering Achievement Award, the OSA Nick Holonyak Award, the SPIE Technical Achievement Award, and the Quantum Devices Award presented at the International Symposium on Compound Semiconductors. He was also the recipient of the S. S. Attwood Award, the Kennedy Family Research Excellence Award, and the Distinguished Faculty Achievement Award presented by The University of Michigan at Ann Arbor.

Linda P. B. Katehi (S'81–M'84–SM'89–F'95) is the Provost and Vice Chancellor for Academic Affairs with the University of Illinois at Urbana-Champaign. Her research is focused on the development and characterization of three-dimensional integration and packaging of integrated circuits with particular emphasis on MEMS devices, high-Q evanescent mode filters and the theoretical and experimental study of planar circuits for hybrid-monolithic and monolithic oscillators, amplifiers, and mixer applications. She has authored and coauthored nine book chapters, 190 papers in refereed journals, and 385 papers in symposia proceedings.

Prof. Katehi is a member of the National Academy of Engineering, the Nominations Committee for the National Medal of Technology, the Kauffman National Panel for Entrepreneurship, the National Science Foundation (NSF) Advisory Committee to the Engineering Directorate, and numerous other engineering and scientific committees.